

## Strain engineering of Dirac cones in graphyne

Gaoxue Wang, Mingsu Si, Ashok Kumar, and Ravindra Pandey

Citation: [Applied Physics Letters](#) **104**, 213107 (2014); doi: 10.1063/1.4880635

View online: <http://dx.doi.org/10.1063/1.4880635>

View Table of Contents: <http://scitation.aip.org/content/aip/journal/apl/104/21?ver=pdfcov>

Published by the [AIP Publishing](#)

---

### Articles you may be interested in

[Engineering of optical polarization based on electronic band structures of A-plane ZnO layers under biaxial strains](#)

J. Appl. Phys. **116**, 113505 (2014); 10.1063/1.4895842

[Tunable double Dirac cone spectrum in bilayer  \$\alpha\$ -graphyne](#)

Appl. Phys. Lett. **103**, 013105 (2013); 10.1063/1.4812977

[Spin splitting in bulk wurtzite AlN under biaxial strain](#)

J. Appl. Phys. **111**, 103716 (2012); 10.1063/1.4720469

[Valley filter in strain engineered graphene](#)

Appl. Phys. Lett. **97**, 043508 (2010); 10.1063/1.3473725

[Valley splitting in strained silicon quantum wells](#)

Appl. Phys. Lett. **84**, 115 (2004); 10.1063/1.1637718

---

An advertisement for Asylum Research Cypher AFMs. The background is dark blue with a film strip graphic on the left. The text is in orange and white. The Oxford Instruments logo is in the bottom right corner.

**Not all AFMs are created equal**  
**Asylum Research Cypher™ AFMs**  
**There's no other AFM like Cypher**

[www.AsylumResearch.com/NoOtherAFMLikeIt](http://www.AsylumResearch.com/NoOtherAFMLikeIt)

**OXFORD**  
INSTRUMENTS  
*The Business of Science®*

## Strain engineering of Dirac cones in graphyne

Gaoxue Wang,<sup>1</sup> Mingsu Si,<sup>2</sup> Ashok Kumar,<sup>1</sup> and Ravindra Pandey<sup>1,a)</sup>

<sup>1</sup>Department of Physics, Michigan Technological University, Houghton, Michigan 49931, USA

<sup>2</sup>Key Laboratory for Magnetism and Magnetic Materials of the Ministry of Education, Lanzhou University, Lanzhou 730000, China

(Received 16 April 2014; accepted 16 May 2014; published online 29 May 2014)

6,6,12-graphyne, one of the two-dimensional carbon allotropes with the rectangular lattice structure, has two kinds of non-equivalent anisotropic Dirac cones in the first Brillouin zone. We show that Dirac cones can be tuned independently by the uniaxial compressive strain applied to graphyne, which induces n-type and p-type self-doping effect, by shifting the energy of the Dirac cones in the opposite directions. On the other hand, application of the tensile strain results into a transition from gapless to finite gap system for the monolayer. For the AB-stacked bilayer, the results predict tunability of Dirac-cones by in-plane strains as well as the strain applied perpendicular to the plane. The group velocities of the Dirac cones show enhancement in the resistance anisotropy for bilayer relative to the case of monolayer. Such tunable and direction-dependent electronic properties predicted for 6,6,12-graphyne make it to be competitive for the next-generation electronic devices at nanoscale. © 2014 AIP Publishing LLC. [<http://dx.doi.org/10.1063/1.4880635>]

Owing to the flexibility of forming  $sp$ ,  $sp^2$ , or  $sp^3$  bonds,<sup>1</sup> carbon can form abundant allotropes including three dimensional (3D) (e.g., diamond and graphite), two dimensional (2D) (e.g., graphene),<sup>2</sup> one dimensional (1D) (e.g., nanotubes<sup>3</sup> and nanoribbons<sup>4</sup>), and even zero dimensional (0D) fullerenes.<sup>5</sup> Among all these allotropes, graphene, the 2D honeycomb carbon sheet, has stimulated extensive studies due to its unconventional electronic properties; the  $\pi$  and  $\pi^*$  bands intersect linearly at the equivalent high symmetry points,  $\mathbf{K}$  and  $\mathbf{K}'$  of the first Brillouin zone (BZ) forming the isotropic Dirac cones near the Fermi energy. The linear dispersion of the bands suggests that excitations in graphene are massless Dirac fermions with speed much smaller than the speed of light, which enables the unusual phenomena of quantum electrodynamics.<sup>1</sup>

Graphyne, another 2D carbon allotrope, which is formed by inserting a carbon triple bond ( $-C\equiv C-$ ) into C–C bond (Figure 1), has attracted increasing attention in recent years. For example, strategies for synthesizing graphyne were proposed.<sup>6,7</sup> Theoretical calculations on  $\alpha$ -,  $\beta$ -, and  $\gamma$ -graphyne were performed predicting the stability and electronic properties.<sup>8</sup> Synthesis of graphdiyne, a 2D carbon allotrope, which has two triple bonds ( $-C\equiv C-$ ) inserted into C–C bond, has also motivated attention on the several forms of 2D carbon allotrope.<sup>9</sup> Very recently, it was predicted that  $\alpha$ -,  $\beta$ -, and 6,6,12-graphyne have graphene-like Dirac cone band structures.<sup>10</sup> Thus, existence of Dirac cones for 6,6,12-graphyne, which has a rectangular lattice, is a significant prediction since it has long been assumed that Dirac cone is unique for the hexagonal 2D materials or topological insulators.<sup>11</sup> Moreover, 6,6,12-graphyne has two nonequivalent anisotropic Dirac cones making it to be even more fascinating than graphene for device applications.

Application of strain is one of the approaches to tailor electronic properties of materials. Strain could be induced by

the mismatch of lattice constant and thermal expansion between the substrate and the film, which has been widely used to achieve tunable properties in functional oxide films.<sup>12,13</sup> In graphene, it has been shown that its Dirac band structure is invariant under a symmetric strain and a band gap could open by applying an asymmetric strain.<sup>14</sup> The tunable energy gap could be realized in a bilayer graphene by changing the strength and direction of strain.<sup>15</sup> Local strain could also be utilized to integrate graphene for all carbon electronics.<sup>16</sup> Experimentally, Kim *et al.* have shown the possibility of applying nearly 30% strain to graphene by the use of stretchable substrates.<sup>17</sup>

Considering the importance of the relationship between strain and the electronic properties of 2D materials, we will investigate such relationship for monolayer and bilayer of 6,6,12-graphyne using density functional theory (DFT) and will show that Dirac cones can be tuned independently with the strain applied to graphyne.

Electronic structure calculations were performed using norm-conserving pseudopotential approach of density functional theory,<sup>18</sup> as implemented in the SIESTA package.<sup>19</sup> In our calculations, van der Waals (vdW) interactions were included in the exchange-correlation functional form to DFT.<sup>20,21</sup> We used  $11 \times 11 \times 1$  Monkhorst-Pack grid<sup>22</sup> for  $k$ -point sampling in the BZ. The mesh cutoff energy is 400 Ry and the vacuum distance perpendicular to the monolayer is

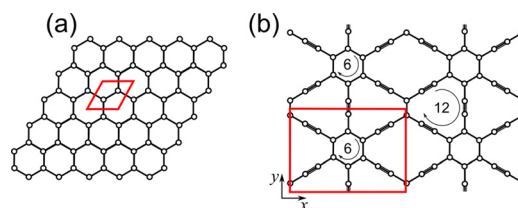


FIG. 1. Schematic representations of (a) graphene and (b) 6,6,12-graphyne. 6,6,12-graphyne is defined by the number of carbon atoms along the rings as shown in (b).

<sup>a)</sup>Author to whom correspondence should be addressed. Electronic mail: [pandey@mtu.edu](mailto:pandey@mtu.edu).

larger than 25 Å in the supercell model employed. The geometric structure was obtained by relaxing all the atoms with residual force smaller than 0.01 eV/Å on each atom.

The 6,6,12-graphyne monolayer is defined by the number of carbon atoms along the rings as shown in Figure 1. In the first BZ, there exist two kinds of anisotropic Dirac cones, which enable the directional dependent transport in the monolayer.<sup>10</sup> One of the Dirac points is slightly above the Fermi energy, and the other is slightly below the Fermi energy suggesting that 6,6,12-graphyne is self-doped.

The (average) length of  $sp^2$  bond is 1.447 Å, and that of the  $sp$  bond is 1.257 Å in the ground state configuration of 6,6,12-graphyne obtained at the vdW-DFT level of theory. The calculated bond lengths are slightly larger than those obtained at DFT level of theory using Perdew-Burke-Ernzerhof (PBE) exchange and correlation functional form.<sup>23</sup> In our case, the cone II has a band gap of 43 meV, which is different from the previous results.<sup>10</sup> This is due to the fact that the exchange-correlation functional form in this study includes the effect of vdW interactions. Note that the representation of the vdW interactions is important in predicting accurate interlayer spacing for bilayers of carbon-based systems.<sup>24</sup>

Figure 2 shows the calculated band structure of the monolayer of 6,6,12-graphyne. The cone I is located at the high symmetric direction from  $\Gamma$  to  $X'$ , and the cone II is at X point. These cones are anisotropic based on the absolute derivative of the  $\pi$  band [right panels of Figs. 2(c) and 2(d)]. The cone I shows linear dispersion with the group velocities of  $v_{k_x} = 0.49 \times 10^6$  m/s and  $v_{k_y} = 0.58 \times 10^6$  m/s, which are about 40% smaller than that of graphene ( $v_F = 0.85 \times 10^6$  m/s).<sup>25,26</sup> The cone II is parabolic near the center of the cone, so the group velocity goes to zero. Note that the group velocity is defined by the derivative of energy dispersion  $v_k = (1/\hbar)(\partial E_k / \partial k)|_{E_k = E_F}$ .

Figure 3 shows the band structure of graphyne with tensile strain applied along  $x$  direction. The strain drives the

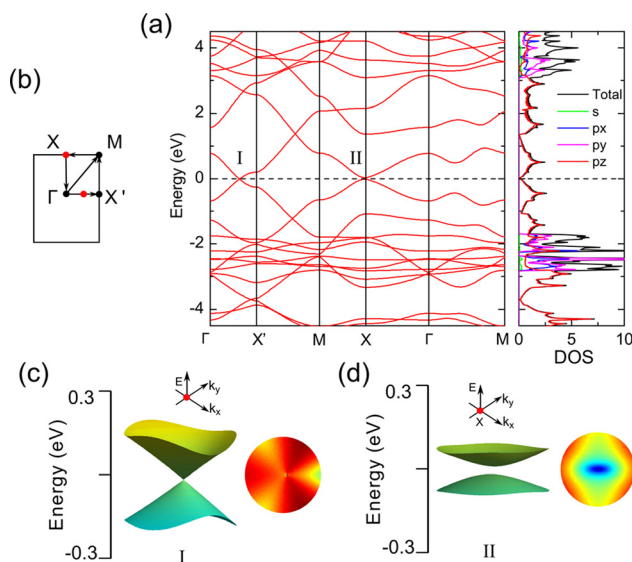


FIG. 2. (a) Band structure of 6,6,12-graphyne monolayer; (b) the illustration of first BZ and high symmetry points; (c) 2D band structure of the cone I (left panel) and the absolute derivative (right panel) of the corresponding  $\pi$  band; and (d) 2D band structure of the cone II (left panel) and the absolute derivative (right panel) of the corresponding  $\pi$  band. Fermi energy is set to zero. The 2D band structure is plotted within a circle of radius  $0.2\pi/a$ .

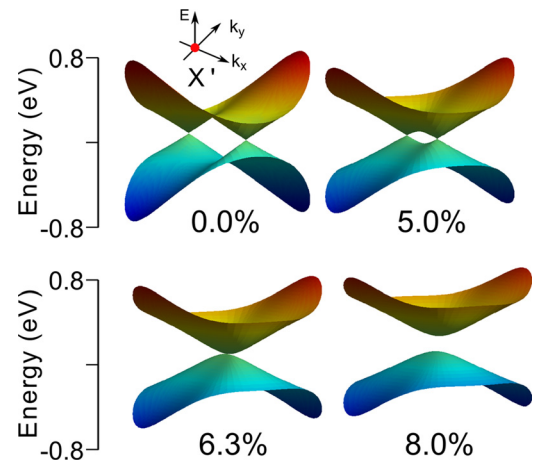


FIG. 3. Variation of the calculated 2D band structures of the cone-I with strain along  $x$ . The band structures are plotted within a circle of radius  $0.5\pi/a$  centered at  $X'$ .

movement of Dirac points in the momentum space. With increasing strain, the cone I moves towards  $X'$ , and the two conical dispersions of the bands around a circle of  $0.5\pi/a$  centered at  $X'$  merge into a single cone at applied strain of 6.3%. The merged cone shows the linear dispersion along  $k_y$  and the parabolic dispersion along  $k_x$  (Figure S1<sup>27</sup>). This is also accompanied by opening of the energy gap for strains larger than 6.3%. Such transition from zero gap to finite gap band structure was also predicted for the pristine graphene under the application of external strain, though the critical strain for the merging of Dirac cones was reported to be larger than 20%.<sup>28–30</sup> Thus, 6,6,12-graphyne could be a potential candidate material to study the merging of Dirac cones without using complex techniques involving molecular graphene<sup>31</sup> or cold atoms.<sup>32</sup> The position of the cone II does not change with tensile strain up to 8% along  $x$  direction. For the tensile strain along  $y$  direction, as shown in Figure S2,<sup>27</sup> gap at the cone II increases, whereas the position of cone I is not affected.

The effects of compressive strain on the band structure of the monolayer are shown in Figure 4. With the compressive strain applied along  $x$  direction, the cone I shifts above Fermi energy, and the cone II shifts below Fermi energy. Thus, shifting of the Dirac points causes n-type doping at the cone I and p-type doping at the cone II. Also, shifting of the cones in the opposite direction results into the enhancement

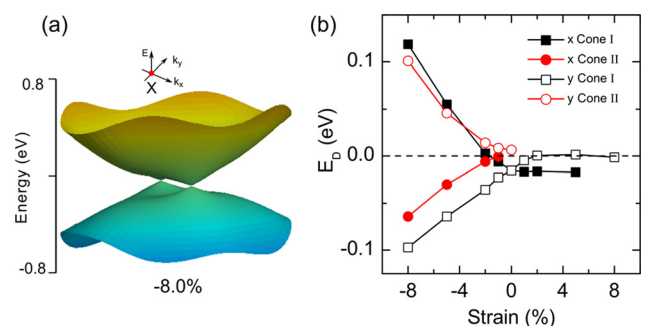


FIG. 4. (a) The calculated 2-D band structure of the cone-II; (b) variation of the energy of the two Dirac points with strain along  $x$  and  $y$ . Fermi energy is set to zero. The band structure is plotted within a circle of radius  $0.5\pi/a$  centered at  $X$ .

of the charge carriers. We notice that the strain induced self-doping effect has also been reported for silicene and germanene<sup>33</sup> for which there only exists one kind of a charge carrier. This is not the case with 6,6,12-graphyne for which both negative and positive charge carriers coexist in the lattice. The Dirac points shift almost linearly with compressive strain up to 10% (Fig. 4(b)), which means the concentration of charge carriers can be tuned effectively. The application of compressive strain along  $y$  direction has similar effects, however, the cone I is p-type doped and the cone II is n-type doped. It is worth noting that due to the change of bond length, the second kind of Dirac cone duplicates with the compressive strain larger than  $-5\%$ , with the center moving away from  $X'$  (Fig. 4(a)).

Since the cone II is parabolic near the center of the cone, its group velocities go to zero when tensile strain is applied. The group velocities appear when the applied compressive strain pushes the cone to be duplicate (Figure 4(a)). For the uniaxial strain along  $x$  direction, the group velocity  $v_{kx}$  of the cone I decreases gradually and goes to zero with the merging of the Dirac cones; the velocity  $v_{ky}$  of the cone I increases slightly and vanishes when the band gap opens up as shown in Figure 5(a). The increased discrepancy between  $v_{kx}$  and  $v_{ky}$  with the tensile strain along  $x$  implies that the anisotropy of the cone I is greatly increased. The anisotropy of the group velocity may lead to the observable resistance anisotropy.<sup>17</sup> For the strain along  $y$ , the group velocities of the cone I nearly remain the same (Figure 5(b)).

Bilayers of graphene-like systems can possess the properties which are not exhibited by monolayers such as tunability of the band gap in graphene bilayer by the external electric field.<sup>34</sup> Also, synthesis of a bilayer is likely to be easier than that of a monolayer; multilayer graphidine was first synthesized before monolayer could be produced.<sup>9</sup> We will now consider 6,6,12-graphyne bilayer focusing on its equilibrium stacking configuration and the effect of strain on its electronic properties.

Considering that the electronic properties of bilayers are highly dependent on the stacking configurations, we have determined the energetically preferred stacking configurations of 6,6,12-graphyne bilayer employing the registry index model.<sup>24</sup> It is well known that the registry index model

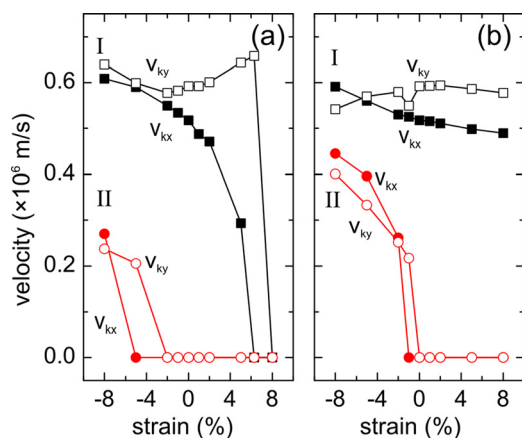


FIG. 5. Variation of the group velocities of  $\pi$  electrons of the cones I and II with the uniaxial strain (a) along  $x$  and (b) along  $y$ .

can capture the main characteristics of the energy surface. For example, it has yielded satisfactory results for graphite and multilayered nanotubes, and bilayer boron nitride (BN).<sup>35</sup> The calculated results find the AB-stacked configuration to be most stable bilayer configuration with the interlayer spacing of  $3.416 \text{ \AA}$  (see supplementary material, Fig. S3 and Table S1 (Ref. 27)). The calculated interlayer distance is consistent with the one predicted for the  $\alpha$ -graphyne.<sup>36</sup>

Figure 6 shows the band structure of the AB stacked bilayer showing the splitting of highly anisotropic Dirac cones (Figures 6(c) and 6(d)) due to appearance of the interlayer interaction in the bilayer system. The group velocities of the cone I are  $v_{kx} = 0.24 \times 10^6 \text{ m/s}$  and  $v_{ky} = 0.55 \times 10^6 \text{ m/s}$  showing the enhancement in anisotropy of resistance for the bilayer relative to that the monolayer. The  $\pi$  and  $\pi^*$  bands at cone II meet together and result into two Dirac points near X (Figure 6(d)). The splitting of Dirac cones is associated with overlapping of  $p_z$  orbitals of the two layers. This is confirmed by taking the interlayer distance to be large enough ( $\sim 6 \text{ \AA}$ ) to exclude interactions between monolayers; the band structure is exactly the same as that of the monolayer [see supplementary material, Figure S4(a)<sup>27</sup>]. On the other hand, a bilayer with a interlayer distance of  $2.5 \text{ \AA}$  shows opening of the band gap of  $43.5 \text{ meV}$  [see supplementary material, Figure S4(b)<sup>27</sup>] due to relatively large overlap of the  $p_z$  orbitals. This implies the possibility of tuning electronic properties with the application of the perpendicular strain to the bilayers.

The effects of the in-plane strains on 6,6,12-graphyne bilayer are similar to the effects predicted for the monolayer. A small tensile strain along  $x$  direction will cause the shifting of the cone I in the BZ. The gap opens up with a larger strain, but the strain along  $x$  has little influence on the cone II [see supplementary material, Figure S5(a)<sup>27</sup>]. Likewise, the uniaxial strain along  $y$  will open up the gap at the cone II, but it does not affect the cone I. The compressive strain shifts Dirac points either above or below Fermi surface

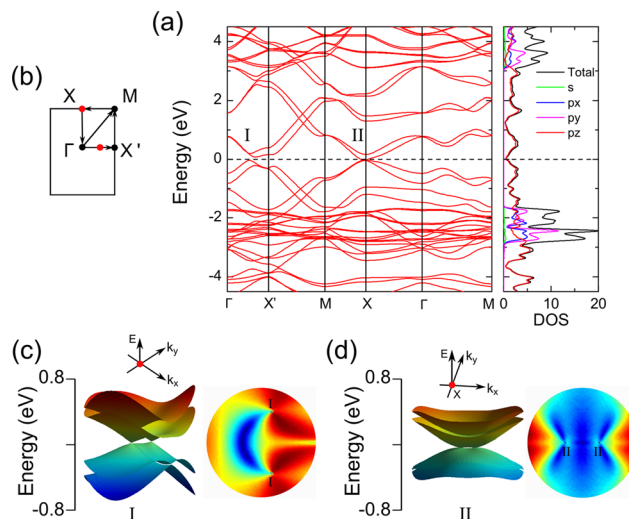


FIG. 6. (a) Band structure of AB-stacked 6,6,12-graphyne bilayer; (b) illustration of the first BZ; (c) 2D band structure around cone I (left panel) and the absolute derivative (right panel) of the corresponding  $\pi$  band; and (d) 2D band structure around cone II (left panel) and the absolute derivative (right panel) of the corresponding  $\pi$  band. Fermi energy is set to zero. The 2D band structure is plotted within a circle of radius  $0.5\pi/a$ .

(Figure S5(b)<sup>27</sup>), which indicates that the self-doping effect in 6,6,12-graphyne bilayer could also be enhanced by a compressive strain.

The elastic properties, which are critical for the strain engineering of electronic properties, can be characterized by Young's modulus and Poisson's ration. As it is ambiguous to define the volume of the sheet with atomic thickness, the in-plane stiffness constant  $C$  is generally used. In the limit of small deformations, the strain energy is simply a quadratic function of strain,<sup>37</sup> so the stiffness constant  $C$  can be expressed as

$$C = \frac{1}{S_0} \frac{\partial^2 E_S}{\partial \varepsilon^2}, \quad (1)$$

where  $S_0$  is the equilibrium area and the strain energy  $E_S$  is the energy difference between the strained and strain relaxed systems. By fitting the strain energy curves within the elastic region, as shown in Figure S6,<sup>27</sup> the stiffness constant can be obtained.

The calculated stiffness constants of 6,6,12-graphyne are 183 and 136 N/m along  $x$  and  $y$  directions, respectively. These values are slightly larger than the values of  $\sim 142$  and  $\sim 112$  N/m (obtained by converting the data obtained by molecular dynamics calculations in units of GPa using the thickness of  $3.2 \text{ \AA}$ ).<sup>38–41</sup> A large anisotropy in stiffness is therefore predicted for the monolayer. Due to the weak interlayer vdW interactions, the stiffness constants for AB stacking bilayer are simply twice that of the monolayer. The stiffness of 6,6,12-graphyne is just one half of the experimental value for graphene ( $340 \pm 40 \text{ N/m}$  (Ref. 42)), which implies that 6,6,12-graphyne is softer than graphene. The softness facilitates the strain engineering of electronic properties and makes the realization of the merging of Dirac cones possible in 2D materials.<sup>28,32,43</sup>

First principles calculations were performed on 6,6,12-graphyne monolayer and bilayer systems. Both monolayer and bilayer systems are semi-metals with Dirac cones in first Brillouin zone. Uniaxial tensile strain along  $x$  will induce shifting of the cone I, and the merging of two conical bands at  $X'$  is predicted. The tensile strain along  $y$  will increase the energy gap at the cone II. The compressive strain shifts the energy of the Dirac points almost linearly, which results into coexistence of positive and negative charge carriers in the lattice. The large anisotropy in stiffness is also being predicted for the monolayer graphyne. The energetically preferred structure of the graphyne bilayer is similar to the Bernal's AB stacking of two adjacent graphene layers. The anisotropy of the Dirac cone is largely enhanced in bilayer, which implies a possibility of increased anisotropy in its electron transport properties. We believe that the predicted tunability of electronic properties makes 6,6,12-graphyne to be candidate 2D material for the next-generation electronic devices at nanoscale.

Helpful discussions with S. Gowtham are acknowledged. RAMA and Superior, high performance computing clusters at Michigan Technological University, were used in obtaining results presented in this paper.

- <sup>1</sup>A. H. Castro Neto, F. Guinea, N. M. R. Peres, K. S. Novoselov, and A. K. Geim, *Rev. Mod. Phys.* **81**(1), 109–162 (2009).
- <sup>2</sup>K. S. Novoselov, A. K. Geim, S. V. Morozov, D. Jiang, Y. Zhang, S. V. Dubonos, I. V. Grigorieva, and A. A. Firsov, *Science* **306**(5696), 666–669 (2004).
- <sup>3</sup>S. J. Tans, A. R. M. Verschueren, and C. Dekker, *Nature* **393**(6680), 49–52 (1998).
- <sup>4</sup>D. V. Kosynkin, A. L. Higginbotham, A. Sinitskii, J. R. Lomeda, A. Dimiev, B. K. Price, and J. M. Tour, *Nature* **458**(7240), 872–876 (2009).
- <sup>5</sup>H. W. Kroto, J. R. Heath, S. C. O'Brien, R. F. Curl, and R. E. Smalley, *Nature* **318**, 216 (1985).
- <sup>6</sup>F. Diederich and M. Kivala, *Adv. Mater.* **22**(7), 803–812 (2010).
- <sup>7</sup>F. Diederich, *Nature* **369**(6477), 199–207 (1994).
- <sup>8</sup>R. H. Baughman, H. Eckhardt, and M. Kertesz, *J. Chem. Phys.* **87**(11), 6687–6699 (1987).
- <sup>9</sup>G. Li, Y. Li, H. Liu, Y. Guo, Y. Li, and D. Zhu, *Chem. Commun.* **46**(19), 3256–3258 (2010).
- <sup>10</sup>D. Malko, C. Neiss, F. Viñes, and A. Görling, *Phys. Rev. Lett.* **108**(8), 086804 (2012).
- <sup>11</sup>H. Zhang, C.-X. Liu, X.-L. Qi, X. Dai, Z. Fang, and S.-C. Zhang, *Nat. Phys.* **5**(6), 438–442 (2009).
- <sup>12</sup>D. G. Schlom, L.-Q. Chen, C.-B. Eom, K. M. Rabe, S. K. Streiffer, and J.-M. Triscone, *Annu. Rev. Mater. Res.* **37**(1), 589–626 (2007).
- <sup>13</sup>A. Chen, Z. Bi, Q. Jia, J. L. MacManus-Driscoll, and H. Wang, *Acta Mater.* **61**(8), 2783–2792 (2013).
- <sup>14</sup>G. Gui, J. Li, and J. Zhong, *Phys. Rev. B* **78**(7), 075435 (2008).
- <sup>15</sup>S.-M. Choi, S.-H. Jhi, and Y.-W. Son, *Nano Lett.* **10**(9), 3486–3489 (2010).
- <sup>16</sup>V. M. Pereira and A. H. Castro Neto, *Phys. Rev. Lett.* **103**(4), 046801 (2009).
- <sup>17</sup>K. S. Kim, Y. Zhao, H. Jang, S. Y. Lee, J. M. Kim, K. S. Kim, J.-H. Ahn, P. Kim, J.-Y. Choi, and B. H. Hong, *Nature* **457**(7230), 706–710 (2009).
- <sup>18</sup>P. Hohenberg and W. Kohn, *Phys. Rev.* **136**(3B), B864–B871 (1964).
- <sup>19</sup>J. M. Soler, E. Artacho, J. D. Gale, A. Garcia, J. Junquera, P. Ordejón, and D. S. Sanchez-Portal, *J. Phys. Condens. Matter* **14**, 2745 (2002).
- <sup>20</sup>M. Dion, H. Rydberg, E. Schröder, D. C. Langreth, and B. I. Lundqvist, *Phys. Rev. Lett.* **92**(24), 246401 (2004).
- <sup>21</sup>G. Román-Pérez and J. M. Soler, *Phys. Rev. Lett.* **103**(9), 096102 (2009).
- <sup>22</sup>H. J. Monkhorst and J. D. Pack, *Phys. Rev. B* **13**(12), 5188–5192 (1976).
- <sup>23</sup>B. G. Kim and H. J. Choi, *Phys. Rev. B* **86**(11), 115435 (2012).
- <sup>24</sup>N. Marom, J. Bernstein, J. Garell, A. Tkatchenko, E. Joselevich, L. Kronik, and O. Hod, *Phys. Rev. Lett.* **105**(4), 046801 (2010).
- <sup>25</sup>P. E. Trevisanutto, C. Giorgetti, L. Reining, M. Ladisa, and V. Olevano, *Phys. Rev. Lett.* **101**(22), 226405 (2008).
- <sup>26</sup>C. Hwang, D. A. Siegel, S.-K. Mo, W. Regan, A. Ismach, Y. Zhang, A. Zettl, and A. Lanzara, *Sci. Rep.* **2**, 590 (2012).
- <sup>27</sup>See supplementary material at <http://dx.doi.org/10.1063/1.4880635> for details.
- <sup>28</sup>V. M. Pereira, A. H. Castro Neto, and N. M. R. Peres, *Phys. Rev. B* **80**(4), 045401 (2009).
- <sup>29</sup>R. de Gail, J. N. Fuchs, M. O. Goerbig, F. Piéchon, and G. Montambaux, *Physica B* **407**(11), 1948–1952 (2012).
- <sup>30</sup>B. Dóra, I. F. Herbut, and R. Moessner, *Phys. Rev. B* **88**(7), 075126 (2013).
- <sup>31</sup>K. K. Gomes, W. Mar, W. Ko, F. Guinea, and H. C. Manoharan, *Nature* **483**(7389), 306–310 (2012).
- <sup>32</sup>L. Tarruell, D. Greif, T. Uehlinger, G. Jotzu, and T. Esslinger, *Nature* **483**(7389), 302–305 (2012).
- <sup>33</sup>Y. Wang and Y. Ding, *Solid State Commun.* **155**, 6–11 (2013).
- <sup>34</sup>E. V. Castro, K. S. Novoselov, S. V. Morozov, N. M. R. Peres, J. M. B. L. dos Santos, J. Nilsson, F. Guinea, A. K. Geim, and A. H. C. Neto, *Phys. Rev. Lett.* **99**(21), 216802 (2007).
- <sup>35</sup>O. Hod, *Phys. Rev. B* **86**(7), 075444 (2012).
- <sup>36</sup>O. Leenaerts, B. Partoens, and F. M. Peeters, *Appl. Phys. Lett.* **103**(1), 013105 (2013).
- <sup>37</sup>C. D. Zeinalipour-Yazdi and C. Christofides, *J. Appl. Phys.* **106**(5), 054318 (2009).
- <sup>38</sup>Q. Yue, S. Chang, J. Kang, S. Qin, and J. Li, *J. Phys. Chem. C* **117**(28), 14804–14811 (2013).
- <sup>39</sup>S. W. Cranford, D. B. Brommer, and M. J. Buehler, *Nanoscale* **4**(24), 7797–7809 (2012).
- <sup>40</sup>S. W. Cranford and M. J. Buehler, *Carbon* **49**(13), 4111–4121 (2011).
- <sup>41</sup>Y. Y. Zhang, Q. X. Pei, and C. M. Wang, *Appl. Phys. Lett.* **101**(8), 081909 (2012).
- <sup>42</sup>C. Lee, X. Wei, J. W. Kysar, and J. Hone, *Science* **321**(5887), 385–388 (2008).
- <sup>43</sup>M. Bellec, U. Kuhl, G. Montambaux, and F. Mortessagne, *Phys. Rev. Lett.* **110**(3), 033902 (2013).